

# RF power consumption emulation optimized with interval valued homotopies

Deogratius Musiige\* , François Anton †, Vital Yatskevich \*, Laulagnet Vincent\*, Darka Mioc ‡, Nguyen Pierre,\*

\*Renesas Mobile Europe

sydhavnsgade 17-19, 2450 Copenhagen

Email:{Deogratius.musiige, Vital.Yatskevich, Vincent.Laulagnet, Pierre.Nguyen}@renesasmobile.com

†Department of Informatics and Mathematical Modeling, The Technical University of Denmark

Building 321, 2800 Kgs. Lyngby, Denmark

Email:fa@imm.dtu.dk ‡National Space Institute, The Technical University of Denmark

Building 348, 2800 Kgs. Lyngby, Denmark

Email:mioc@space.dtu.dk

**Abstract**—This paper presents a methodology towards the emulation of the electrical power consumption of the RF device during the cellular phone/handset transmission mode using the LTE technology. The emulation methodology takes the physical environmental variables and the logical interface between the baseband and the RF system as inputs to compute the emulated power dissipation of the RF device. The emulated power, in between the measured points corresponding to the discrete values of the logical interface parameters is computed as a polynomial interpolation using polynomial basis functions. The evaluation of polynomial and spline curve fitting models showed a respective divergence (test error) of 8% and 0.02% from the physically measured power consumption. The precisions of the instruments used for the physical measurements have been modeled as intervals. We have been able to model the power consumption of the RF device operating at 5MHz using homotopy between 2 continuous power consumptions of the RF device operating at the bandwidths 3MHz and 10MHz.

**Keywords**—Radio frequency, High Power Amplifier, Baseband, LTE, Power, Emulation, Homotopy, Interval analysis, Tx power, Register-Transfer Level.

## I. INTRODUCTION

The rapidly growing wireless telecommunication technology demands high data rates at low costs and low power consumption. Sophisticated modulation and access schemes such as the *Orthogonal Frequency Division Multiplex (OFDM)* in *Long Term Evolution (LTE)* [19] (which is the telecommunication technology used in this paper) have been introduced to meet the high data rates demand, but the low cost and power consumption criteria are much influenced by the *Base Band (BB)* and *RF (Radio Frequency)* devices. The RF device consists of the *RFIC (Radio Frequency Integrated Circuit)* and the *HPA (High Power Amplifier)*.

The BB and the RF devices determine the electrical power consumption and the emitted radiation during the cellular phone or wireless handset transmission/reception of data. The focal point of this paper is the optimization of the dissipated electrical power of the RF devices before the production of the integrated circuits. Thus, we emulate the power consumption behaviors of the RF device, in order to analyze the dissipated power where the hot spots can be identified and approaches towards their minimization taken during the design of the

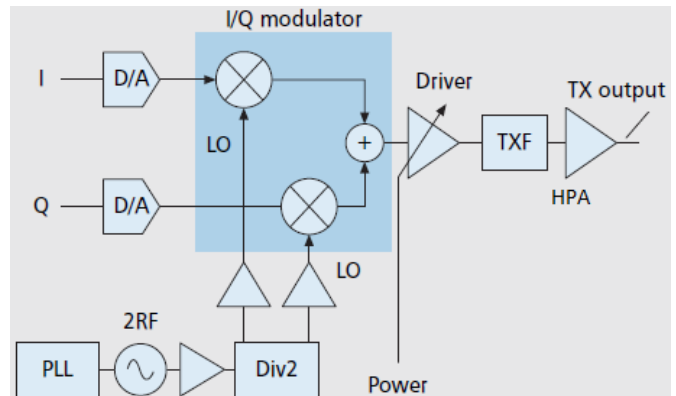


Fig. 1 Direct up conversion transmitter RF device architecture(modified from [17])

cellular phones and wireless handsets. The emulation approach is preferable for its close link to the physics of the real device in contrast to simulation approaches.

### A. RF devices

The RF device is responsible for mixing the digital coded and modulated data from the BB with a RF signal making it transmittable in a desired frequency band. Figure 1 depicts the architecture of a direct up conversion topology of the RF device [17] used for the analysis in this paper. In the RF device topology, the digital in phase (I) and quadrature (Q) data from the BB are analog converted, mixed up with a RF signal from the *Local Oscillator (LO)* and amplified by the HPA. The resultant signal is forwarded to the antenna devices for transmission. In Figure 1, the PLL (*Phase Locked Loop*) produces the 2RF ( $2 \times$  *Radio Frequency*) which is divided by 2 (Div2) and forwarded to the LO and the TXF (*TX Filter*) attenuates frequencies out of the desired frequency range.

This architecture based on the direct up conversion transmitter topology is much desired for its simplicity and high integration. The necessary number of desired external components compared to other architectures [17] is minimal thus a low power consumption, small chip size and low cost. Though

this architecture is largely desired for its simplicity, it does have a problem with the local oscillator distortion by the HPA. This problem occurs when the output of the HPA couples back to the oscillator [22]. The oscillator tends to shift toward the frequency of this external stimulus because the HPA output is a modulated waveform having a higher power and a spectrum centered around the frequency of the oscillator [22]. This phenomenon is referred to as injection pulling or injection locking. This problem can be alleviated if the spectrum of both the oscillators and the HPA output are distant in the frequency-magnitude domain by utilizing either offset local oscillators or a 2 step architecture.

There are 2 other RF device architectures for consideration:

- 1) The polar architectures use the phase and magnitude information to form the complex transmitter signal in contrast to the mixer and PLL(Phase Locked Loop) based architectures, which employ rectangular modulation. The polar architecture is the most power efficient transceiver architecture according to the study conducted in [24] for the WIMAX (*Worldwide Interoperability for Microwave Access*) technology which is very close to the LTE technology. This architecture is however undesired due to its practical imperfections leading to spectral regrowth, increased *Error Vector Magnitude (EVM)* and link performance loss [17].
- 2) The LINC (*Linear amplifier with Nonlinear Components*) transmitter architectures employ nonlinear components to form an efficient linear amplifier. This architecture enables us to have nonlinear high efficiency HPA's at the price of low integration and enlarged chip size. However, compared with the direct conversion and polar transmitters, this architecture is impractical and highly costly [24].

During the RF transmitter design, the choice of a RF architecture is indeed contingent upon the desired *Peak to average power ratio (PAPR)*, bandwidth of both baseband and modulated RF signals, Cost, *ACLR (Adjacent Channel leakage Ratio)*, EVM and area efficiency. The choice of the transmitter architecture and technology solution is also contingent on the performance of the corresponding receiver solutions as in practical terms, the transmitter and receiver do share the same integrated circuit.

### B. The LTE technology

The LTE technology [19] is the newest generation of cellular phone and wireless handset technology and is intended to reach high peak data rates of 100Mbps down link and 50Mbps uplink (Release 8), low latency, high radio efficiency, low cost and high mobility characteristics. The LTE technology is made up of 3 fundamental technologies:

- The *Orthogonal Frequency Division Multiple Access (OFDMA)* used for downlink.
- The *Single Carrier- Frequency Division Multiple Access (SC-FDMA)* used for uplink.
- The *Multiple input Multiple output (MIMO)* used for both downlink and uplink

1) *The OFDMA technology:* The OFDMA is a technology that has evolved from *Frequency Division Multiplexing (FDM)* and *Orthogonal Frequency Division Multiplexing (OFDM)* with the inclusion of Time Division Multiplex Access (TDMA) principles. The FDM technology was the first multi carrier technology and it is widely used in television transmitters. The main drawback of this technology was its spectral inefficiency due to the requirement of guard bands between carriers. Consequently, the OFDM technology was proposed which is also based on the multi-carrier principles but eradicated the necessity of guard bands in the FDM technology by utilizing orthogonal sub channels [19]. The orthogonality is achieved by choosing the spacing between the sub-carriers such that at the sampling point of the individual sub-carriers, the other sub-carriers have 0 values. The OFDM technology solely allow a single user on a channel at any given time. For a system using OFDM modulation to accommodate multiple users on the same channel, TDMA has to be applied so that each user can have a share of the channel for a given TDMA slot. In order to fully utilize the capacity of the channel, the diversification of the channel in time and frequency domain is applied. Thus, the 2 LTE technologies OFDM and OFDMA differ in that OFDM is a modulation scheme while OFDMA is the access scheme used to effectively diversify the resources (OFDM channels) among different users according to their bandwidth necessities [19].

2) *The SC-FDMA technology:* In the uplink direction of the LTE system, the SC-FDMA technology is used in contrast to the OFDMA technology used in the downlink direction. It would have been very practical to use the OFDMA technology in both directions. However, due to OFDMA's high requirement of Peak-to-Average Power Ratio (PAPR) and the demand for power efficient hand held devices, OFDMA is to be used in the base station where we do not have limited resources in terms of power. The SC-FDMA utilizes the desirable characteristics of the OFDM and the low PAPR of single-carrier transmission schemes to make an efficient LTE uplink.

3) *The MIMO technology:* MIMO uses spatial multiplexing, beam forming and pre-coding [23] principles, where different TX's are sent from different antennas with different data streams in the transmitter at the same time. On the receiver side, the data streams are detected by signal processing means utilizing the propagation channel characteristics.

4) *LTE technological influence on power consumption:* The LTE is targeted to provide 100Mbit/s and 50Mbit/s for downlink and uplink respectively for category 3 and slightly higher for category 5. It is the power consumption during uplink transmission that is of interest in this paper. Thus, it is the amount of watts consumed per throughput bit. In frequency domain, the OFDMA transmission consists of several parallel sub carriers where the time domain equivalent is a sum of these sub carriers (sinusoids). The geometrical envelope of the time domain waveform representation tends to vary strongly leading to a very high PAPR. The PAPR of this magnitude leads to a large back-off requirement in the design of the HPAs and this is the reason that OFDMA is only to be used in basestations in the LTE technology. On the other hand, the usage of SC-

FDMA in the uplink is a very good choice in terms of PAPR and HPA efficiency, as the resultant waveform of SC-FDMA behaves as a single sinusoid with low PAPR. Hence, a very good HPA efficiency for the uplink which is very desired as cellular phones and wireless devices run on batteries. *Crest factor reduction (CRF)* schemes have been proposed as in [26] to reduce the OFDM PAPR though they have not been applied in the LTE yet.

The LTE technology MIMO and the beam forming and pre-processing signal processing techniques are very beneficial for power consumption. Indeed, with the MIMO technology, we do have a data rate increase of some factors depending on the MIMO configuration. Moreover the necessary coding is also reduced as different received signals are used to estimate the transmitted signal. Hence, the more data we are capable of transmitting in the same amount of time and power, the more power is being saved. A beam forming technique which ensures directional transmission is also employed in LTE.

### C. Overview of power emulation methodologies

The new paradigm for power estimation called power emulation was introduced in [12], [13] for *RTL (Register Transfer Level)* power estimation. In this methodology, each RTL component is associated with a power model depicted in Figure 2 that computes its emulated power consumption. The operations of the power model can be mathematically expressed as:

$$Power = \sum_{x=1}^N XOR(in_x, Q) \times Coeff\_x$$

where N is the number of inputs/outputs of the component of interest.

The power model takes the values of the inputs/outputs of the RTL component as inputs and utilizes a flip-flop to save the previous values. At a given clocking by the "POW\_STROBE", the current and previous values of say *in1* (in Figure 2) are evaluated for a binary transition by the XOR operation and the product AND gated with the power coefficient associated to the *in1* transition to produce the corresponding power consumption.

The corresponding work on power emulation [8], [18] focuses on the applicability and optimization of the power emulation methodology based on the power model introduced in [12], [13]. However, to our knowledge, there have not been published any research on the power emulation of analog devices. The defined power model in [13] that forms the core of the available power emulation methodologies targets the RTL designs which are digital in contrast to our fully analog RF device. This paper is presenting a methodology for emulating the power consumption of an analog device (RF device).

### D. Power emulation

The power emulation methodologies outlined in the overview section can be applied for the power emulation of the digital BB from the RTL level of abstraction. In these

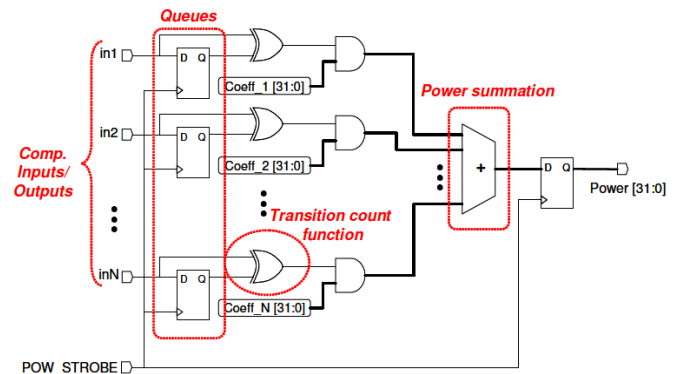


Fig. 2 Power model (modified from [13])

methodologies, the emulated power is computed as the sum of the products of the observed activity and the power coefficients of the RTL components in the design. However, since the RF device is entirely analog, similar power emulation approaches can not be applied. For that purpose, we scrutinized the physical environmental variables and the logical interface between the BB and the RF device for the parameters that might affect the dissipated power. We conducted the physical power dissipation measurements as a function of the physical environmental variables and the logical interface between the RF device and BB on a specific RF device. The physical power measurements are analyzed and a model reflecting their behaviors as a function of the logical interface and the physical environmental variables computed.

The RF device emulation methodology presented in this paper computes the emulated power in between measured points as a polynomial interpolation using polynomial basis functions [9] which take the logical interface parameters as inputs. The influence of the only considered physical environment variable (the temperature) on the emulated power is modeled as a homotopy. Indeed, homotopies have been used successfully for modeling continuously changing physical phenomena as homotopy is a continuous deformation (see section III).

This paper is organized as follows. The next section (II) covers RF device power emulation followed by homotopies and interval analysis in section III. In section IV the paper is presenting the evaluation of the RF device - BB logical interface towards power consumption followed by further work and conclusion in sections V and VI.

## II. RF DEVICE POWER EMULATION

A power emulation system that takes the physical environmental variables and the logical interface parameters between the *BBIC (Baseband Integrated Circuit)* and the RF device via the *DIGRF* interface [7] and *HDMI (High-Definition Multimedia Interface)* as input to produce the power consumption of a specific RF device during run time is depicted in Figure 3. The essence in this power emulation methodology, is the computation of the RF device power consumption for the combinations of the logical interface parameters and the physical environmental variables at any given time of operation. The "Parameter extractor" module is a collection of parallel

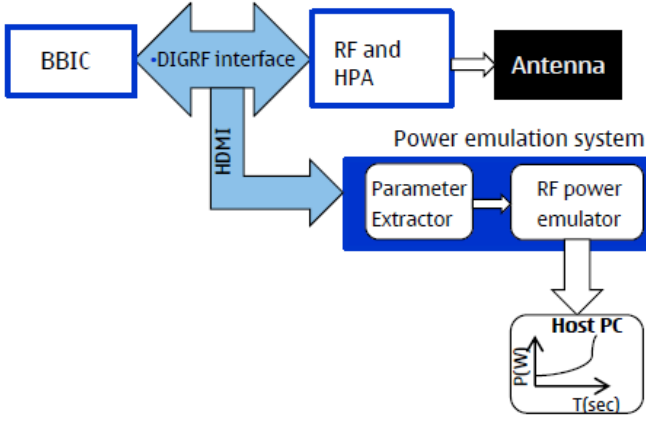


Fig. 3 RF power emulation system

latches used for retrieving and withholding the runtime values of the logical interface parameters and physical environmental variables. The operations of the power emulator as a function of time  $t$  and the physical environmental variable temperature  $T$  can be expressed as:

$$P(t, T) = \sum_{i=0}^{M-1} w_j(t, T) \times \phi_j(x(t))$$

$$P(t, T) = \sum_{i=0}^{M-1} w_j(t, T) \times \phi_j(x(t)) \quad (1)$$

where  $M$  is the number of coefficients and  $\phi(\cdot)$  is the basis function expressing the features of the input data  $x(t)$  which consists of the logical interface parameters.

#### A. RF device - BB Logical interface

The logical interface parameters that influence power consumption are determined by the characteristics of the uplink *SC-FDMA* (Single Carrier-Frequency Division Multiplex Access) signal [4] after the up conversion operations of the RF device (the signal at the antenna switch). The LTE uplink signal  $S_l(t)$  for  $0 \leq t < (N_{CP,l} + N) \times T_s$  is defined as:

$$S_l(t) = \sum_{k=-\lfloor N_{RB}^{UL} N_{SC}^{RB} / 2 \rfloor}^{\lfloor N_{RB}^{UL} N_{SC}^{RB} / 2 \rfloor} a_{k(-)} \times e^{j2\pi(k+0.5)\Delta f(t-N_{CP,l}T_s)} \quad (2)$$

where:

$N_{SC}^{RB}$  is the resource block size in the frequency domain, expressed as a number of sub carriers

$N_{RB}^{UL}$  is the uplink bandwidth configuration, expressed in multiples of  $N_{SC}^{RB}$

$a_{k(-)}$  is the content of the resource element (k,l)

$N_{CP,l}$  is the downlink cyclic prefix length for OFDM symbol  $l$  in a slot

$N = 2048$

$\Delta f = 15KHz$

The product of the  $S_l(t)$  signal after the RF device can be expressed in compact form:

$$RF(t) = A \times Re\{S_l(t)\} \cos(2\pi f_c t) - B \times Im\{S_l(t)\} \sin(2\pi f_c t) \quad (3)$$

where  $A$  and  $B$  are the amplitudes and  $f_c$  is the carrier frequency. The characteristics of the  $RF(t)$  signal defining the logical interface [4] parameters from the LTE technological point of view are:

- the uplink bandwidth  $\in [1.4 \ 3 \ 5 \ 10 \ 15 \ 20]$  MHz,
- the modulation (encompassed in the content of resource blocks) schemes QPSK, 16QAM and 64 QAM,
- the TX power in form of the  $RF(t)$  signal amplitude (this is defined to be between -40 and 23 dBm),
- the carrier frequency  $f_c$  (the defined LTE bands).

### III. HOMOTOPIES AND INTERVAL ANALYSIS

An homotopy is a continuous deformation of geometric figures or paths or more generally functions: a function (or a path, or a geometric figure) is continuously deformed into another one [6]. Such functions or paths are then considered equivalent: i.e., homotopic. Originally, homotopy was used as a tool to decide whether two paths with same end-points would lead to the same result of integration. The use of homotopies can be tracked back to works of Poincaré (1881-1886), Klein (1882-1883), and Berstein (1910) [6].

A homotopy is defined as a continuous map between two continuous functions in a topological space. A homotopy can, therefore, be viewed as a *continuous deformation*. The use of deformations to solve non-linear systems of equations may be traced back at least to Lahaye (1934) [6].

A homotopy between two continuous functions  $f_0$  and  $f_1$  from a topological space  $\mathcal{X}$  to a topological space  $\mathcal{Y}$  is defined as a continuous map  $\mathcal{H} : \mathcal{X} \times [0, 1] \rightarrow \mathcal{Y}$  from the product space  $\mathcal{X}$  with the unit interval  $[0, 1]$  to  $\mathcal{Y}$  such that

$$\mathcal{H}(\mathbf{x}, 0) = f_0, \text{ and} \quad (4)$$

$$\mathcal{H}(\mathbf{x}, 1) = f_1, \quad (5)$$

where  $\mathbf{x} \in \mathcal{X}$ . The second parameter of  $\mathcal{H}$ , also called the *homotopy parameter*, allows for a continuous deformation of  $f_0$  to  $f_1$  [6].

Two continuous functions  $f_0$  and  $f_1$  are said to be *homotopic*, denoted by  $f_0 \simeq f_1$ , if and only if there is a homotopy  $\mathcal{H}$  taking  $f_0$  to  $f_1$ . Being homotopic is an equivalence relation on the set  $C(\mathcal{X}, \mathcal{Y})$  of all continuous functions from  $\mathcal{X}$  to  $\mathcal{Y}$ .

We use homotopies in order to reconstruct the unknown function of the consumed power of several power influencing variables (logical interface parameters and the physical environmental variables) from the measured values obtained by fixing one variable (that will be used as homotopy parameter) and varying another variable (or possibly several other variables). In this way, we study the projections of the graph of that function of the consumed power on lower dimensional spaces (usually 2 dimensional spaces) corresponding to limit values of the range of the RF device power influencing variable used as homotopy parameter (e.g. carrier frequency or temperature). The homotopies are specifically very strong in the modeling

of continuous variables in our case the physical environmental variables temperature. In the case of the temperature, a continuous map  $\mathcal{H} : \mathcal{X} \times \lambda \rightarrow \mathcal{Y}$ ,  $\lambda \in [0, 1]$  can be used to model the power consumption as a function of temperature in the defined temperature range ( $-10^{\circ}\text{C}$  to  $+55^{\circ}\text{C}$ ) [1]. The homotopy parameter  $\lambda$  would be set as  $\lambda = 0$  and  $\lambda = 1$  for the power consumptions at temperatures  $-10^{\circ}\text{C}$  and  $+55^{\circ}\text{C}$  respectively and all the power consumptions in this range are on the homotopy curve as  $\lambda$  goes from 0 to 1. For the measurement conducted in this paper, the temperature is assumed to be constant.

Interval analysis is a well-known method for computing bounds of a function, being given bounds on the variables of that function [15]. The basic mathematical object in interval analysis is the interval instead of the variable. The operators need to be redefined to operate on intervals instead of local variables. This leads to an interval arithmetic. In the same way, most usual mathematical functions are redefined by an interval equivalent. Interval analysis allows one to certify computations on intervals by providing bounds on the results. The uncertainty of each measure can be represented using an interval defined either by a lower bound and an upper bound or a midpoint value and a radius. The uncertainty of the consumed power as a function of a variable (say bandwidth) can be represented by an upper bound plot and a lower bound plot. The consumed power in between the measured points can be interpolated linearly or by using cubic splines. The theoretical assumption that the consumed power is monotonically increasing with respect to the defined power influencing variables is tested by computing the intersection of the areas between the lower bound plots and the upper bound plots corresponding to the limit values of the homotopy parameter.

In Figure 4, the convex homotopy [6]  $H(x, \lambda) = \lambda^{\alpha}G(x) + (1 - \lambda)^{\alpha}F(x)$  is used to estimate the power consumption of the RF device operating at a 5MHz bandwidth. In the convex homotopy,  $\lambda \in [0, 1]$ ,  $G(x)$  and  $F(x)$  are power consumptions of the RF device operating at 10MHz and 3MHz bandwidths respectively and  $\alpha$  is appropriately chosen to represent the curvature of  $G(x)$  and  $F(x)$ . The value of  $\alpha$  has been accordingly set in order to evaluate the convex homotopy  $H(x, \lambda)$  as a linear, non-linear and quadratically varying non-linear function.

With the given three behaviors of the convex homotopy as a function of  $\alpha$ ,  $H(x, 0.286) = 0.286^{\alpha}G(x) + 0.714^{\alpha}F(x)$  estimates the power consumption of the RF device operating at 5MHz. It can be observed (in Figure 4) that the non-linear ( $\alpha = 0.9$ ) and the quadratically varying non-linear convex homotopies have acceptable estimates when compared to the measured 5MHz power consumption. The y-axis in Figure 4 and all the corresponding graphs in the paper are disguised due to the confidentiality of the exact power figures.

#### IV. EVALUATION OF THE RF DEVICE - BB LOGICAL INTERFACE TOWARDS POWER CONSUMPTION

A transceiver prototype supporting the LTE technology with the BB and RF device was used for the analysis of the logical

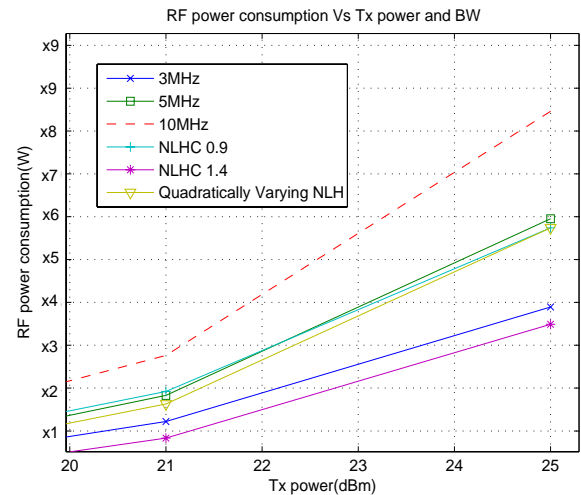


Fig. 4 Behaviors of different homotopies

interface parameters defined in the “RF-BB Logical interface” section towards power consumption (only the bandwidth and TX power are analyzed in this paper). The prototype was connected to a signal analyzer [5] capable of measuring the channel power of the signal (see Equation 6) at the antenna port. The channel power of the signal at the antenna port is defined as:

$$P = \int_{F_1}^{F_2} G(f)df + \int_{-F_1}^{-F_2} G(f)df \quad (6)$$

where  $G(f)$  is the power spectral density of the signal at the antenna port [10], frequencies  $F_1$  and  $F_2$  define the operational frequency band and  $f$  is the continuous frequency in the operational frequency band.

For the power consumption of the RF device, a resistor was inserted in its voltage supply line to get the current by applying Ohm’s law which states that for a voltage  $V_d$  across a circuit of resistance  $R$ , the current over this circuit is  $I = V_d/R$  [11], [16]. By incorporating this current into Joule’s law [25] of the dissipated power, the power consumption of the RF device could be computed as  $P = V \times I$ . NI LabView’s [2] flexible-resolution digitizer was applied for the measurement of the voltage difference over the resistor. The measurement uncertainties due to the precisions in the voltage supply device [3], resistance and NI labView’s flexible-resolution digitalizer were modeled using intervals [15]. Thus, the RF device power consumption is represented in form of intervals specified by lower and upper bounds:

$$[P \bar{P}] = [V \bar{V}] \times ([V_d \bar{V}_d]) \times \left[ \frac{1}{R} \frac{1}{R} \right] \quad (7)$$

where  $V$  is the voltage source and  $V_d$  the voltage difference over the resistor  $R$ .

The influence of the bandwidth as a function of TX power  $P$  is depicted in Figure 5.

Figure 5 shows that the bandwidth has minimal influence on the RF device (used in this experiment) power consumption.

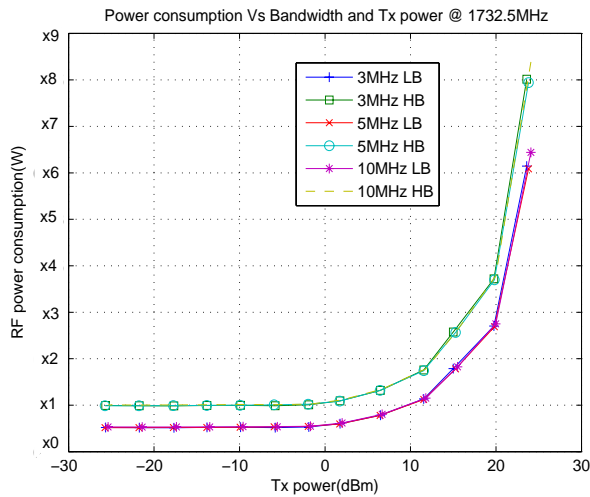


Fig. 5 Measured RF device power consumption

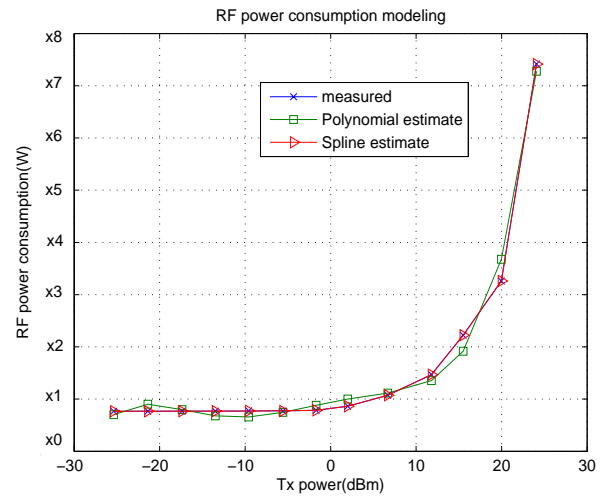


Fig. 6 The emulated power

For the analysis of this behavior, it has been proven that the power consumption of the RF device has 2 main sources:

- 1) The RFIC,
- 2) The HPA.

For the RFIC contribution, power consumption as a function of bandwidth and frequency is technology dependent [20]. Faster processes tend to reduce power consumption at high frequencies while at low frequencies a slow and fast technology might provide a nearly equivalent performance. The signal bandwidth has also a similar relation because most integrated filters use feedback circuits with operational amplifiers whose bandwidth depend on the technology. However, as the RFIC generally consumes less power and at high TX powers the HPA consumes up to 5 times more power than the RFIC [19], the power consumption trends of the RF device are defined by the HPA.

The power consumption of the HPA is very design dependent considering the *Power Added Efficiency (PAE)* as a function of the frequency for a wide band power amplifier [21], [14] (as the one used for the measurements). Given a PAE versus frequency sweep for a wide band power amplifier, the proportion of the high resolution of frequency (GHz, on the frequency axis) compared to the maximum bandwidth (10MHz used in the measurements) is 1% and less than the uncertainty in the measurements (see equation 8), making the PAE difference in a 3, 5 and 10 MHz bandwidth insignificant. Thus explaining why the difference between the RF device power consumptions operating at 3, 5 and 10 MHz is relatively small.

$$\Delta P(Vd) = \frac{(\Delta V \times Vd + V \times \Delta Vd) \times R + (V \times Vd) \times \Delta R}{R^2} \quad (8)$$

## V. RF DEVICE EMULATION ILLUSTRATION OF A SPECIFIC SCENARIO

Figure 5 depicts the power consumption of the RF device as a function of bandwidth and TX power at a carrier

frequency of 1732.5MHz modulated with QPSK. Thus, at a carrier frequency of 1732.5MHz, a scenario with a constant bandwidth 10MHz and QPSK modulation with varying TX power can be assumed. The emulation of this scenario would require the power emulation module in Figure 3 to make the operations expressed in Equation 1. The input data  $x$  in the scenario is shown in the matrix  $X$  below where  $TxP_{i=1...13} \in [-25.38 \ 24.08]$ ,  $f_c = 1732.5MHz$ ,  $BW = 10MHz$  and the QPSK modulation denoted as 1:

$$\mathbf{X} = \begin{pmatrix} TxP_1 & TxP_2 & \dots & TxP_{13} \\ f_c & f_c & \dots & f_c \\ BW & BW & \dots & BW \\ 1 & 1 & \dots & 1 \end{pmatrix}$$

Due to the fact that in this scenario the carrier frequency, bandwidth and the modulation are constant as shown in matrix  $X$ , only the TX power in the first row is considered for the modeling of the RF device power consumption. It can be observed that the RF device power consumption depicted in Figure 5 behaves as a polynomial, hence polynomial and spline (which is made up of piecewise polynomials) fitting methods were evaluated. For polynomial curve fitting, there had to be defined a degree  $d$  and vector  $w$  of  $1 \times d + 1$  coefficients such that the modeled power would be defined as:

$$\hat{P}(t, T) = \begin{pmatrix} 1 & TxP_1 & TxP_1^2 & \dots & TxP_1^d \\ 1 & TxP_2 & TxP_2^2 & \dots & TxP_2^d \\ \vdots & \vdots & \vdots & \ddots & \vdots \\ 1 & TxP_N & TxP_N^2 & \dots & TxP_N^d \end{pmatrix} \begin{pmatrix} w_0 \\ w_1 \\ w_2 \\ \vdots \\ w_d \end{pmatrix}$$

where  $TxP$  is the TX power of length  $N$  and the least mean squares approach is applied to solve for the vector of coefficients.

In Figure 6, the performances of the polynomial and spline fitting can be observed. The polynomial fitting method of degree 6 has a maximum divergence (test error [9]) of 8%

from the measured RF device power consumption while the spline method has a divergence of 0.02%. The selection of the fitting methodology to be applied would be a trade off between the desired accuracy and complexity.

## VI. FURTHER WORK

The emulation methodology presented in this paper takes the logical interface and the physical environmental variables as the input parameters to compute the emulated power consumption. There are 2 future targets of this work:

- the generalization of the power consumption emulator where any RF device can be emulated.
- an emulation model that both emulates the power consumption of the RF device and the radiation emitted during the operations of the RF device. Thus, the subsequent work is to analyze the influence of logical interface parameters and the physical environmental variables on the emitted radiation.

## VII. CONCLUSION

The available work on emulation [12], [13], [8], [18] targets digital designs at the RTL level of abstraction. This paper has presented an emulation methodology towards the emulation of the power consumption of the analog RF device. This methodology computes the emulated power consumption of the RF device as a polynomial interpolation using polynomial basis functions, taking the RF device - BB logical interface as inputs, and the pre-defined models. The RF device power emulation methodology has been evaluated with a test error of 8% and 0.02% for polynomial and spline models respectively. By utilizing the power emulation methodology in [12], [13] for emulating the digital BB and the methodology in this paper, we can emulate the power consumption of the whole transceiver chain during runtime. In addition, given the fact that power consumption emulation can be performed during the design phase of the BB and RF devices, power analysis can be conducted where hot spots are found and actions towards their minimization taken. Thus, by incorporating the available emulation methodologies for the BB and the methodology presented in this paper, BB and RF devices designs and operational scheduling can be implemented towards optimal power usage.

## REFERENCES

- [1] *3GPP Technical Specification 36.101*, v8.0.0 edition, 2007.
- [2] *NI PXI/PCI-5922 Specifications*, 2007.
- [3] *Programmable DC Power Supplies*, 2007.
- [4] *3GPP Technical Specification 36.211*, v8.9.0 edition, 2009.
- [5] *Rohde & Schwarz Signal analyzer*, 2010.
- [6] E. L. Allgower and K. Georg. *Numerical continuation methods: an introduction*. Springer-Verlag New York, Inc. New York, NY, USA, 1990.
- [7] MIPI Alliance. <http://www.mipi.org/specifications/digrfsm-specifications>, 2011.
- [8] C. Bachmann, A. Genser, C. Steger, R. Weiss, and J. Haid. Automated power characterization for run-time power emulation of soc designs. In *Digital System Design: Architectures, Methods and Tools (DSD), 2010 13th Euromicro Conference on*, pages 587 –594, 2010.
- [9] Christopher M. Bishop. *Pattern Recognition and Machine Learning*. Springer, 2006.
- [10] B.Sklar. *Digital Communications, Fundamentals and applications*. Prentice hall PTR, 2001.
- [11] C. V. Clarence. *Electrical Engineering: The Theory and Characteristics of electrical Circuits and Machinery*. McGraw-Hill, 1917.
- [12] J. Coburn, S. Ravi, and A. Raghunathan. Hardware accelerated power estimation. In *Design, Automation and Test in Europe, 2005. Proceedings*, pages 528 – 529 Vol. 1, 2005.
- [13] J. Coburn, S. Ravi, and A. Raghunathan. Power emulation: a new paradigm for power estimation. In *Design Automation Conference, 2005. Proceedings. 42nd*, pages 700 – 705, 2005.
- [14] Xian Cui. *Efficient radio frequency power amplifiers for wireless communication*. PhD thesis, The Ohio State University, 2007.
- [15] R.Baker Kearfott E. Ramon Moore and Michael J. Cloud. *Introduction to interval analysis*. SIAM (Society for Industrial and Applied Mathematics Philadelphia), 2009.
- [16] N. G. Ejuh and G. H. Tyler. *McGraw-Hill's Engineering companion*. McGraw-Hill, 2002.
- [17] J. Groe. Polar transmitters for wireless communications. *Communications Magazine, IEEE*, 45(9):58 –63, 2007.
- [18] J. Haid, C. Bachmann, A. Genser, C. Steger, and R. Weiss. Power emulation: Methodology and applications for hw/sw power optimization. In *Formal Methods and Models for Codesign (MEMOCODE), 2010 8th IEEE/ACM International Conference on*, pages 133 –138, 2010.
- [19] Harri Holma and Antti Toskala. *LTE for UMTS: OFDMA and SC-FDMA Based Radio Access*. Wiley & Sons, 2008.
- [20] M. Racanelli, S. Voinescu, and P. Kempf. High performance sige bicmos technology. In *Wireless Communications and Applied Computational Electromagnetics, 2005. IEEE/ACES International Conference on*, pages 430 – 434, 2005.
- [21] V. Radisic, Y. Qian, and T. Itoh. Broad-band power amplifier using dielectric photonic bandgap structure. *Microwave and Guided Wave Letters, IEEE*, 8(1):13 –14, January 1998.
- [22] B. Razavi. Rf transmitter architectures and circuits. In *Custom Integrated Circuits, 1999. Proceedings of the IEEE 1999*, 1999.
- [23] C.B. Ribeiro, K. Hugl, M. Lampinen, and M. Kuusela. Performance of linear multi-user mimo precoding in lte system. In *Wireless Pervasive Computing, 2008. ISWPC 2008. 3rd International Symposium on*, pages 410 –414, May 2008.
- [24] Liang Rong, F. Jonsson, Lirong Zheng, M. Carlsson, and C. Hedenas. Rf transmitter architecture investigation for power efficient mobile wimax applications. In *System-on-Chip, 2008. SOC 2008. International Symposium on*, pages 1 –4, nov. 2008.
- [25] F. M. William. *Principles of Physics: Designed for Use as a Textbook of General Physics*. University of Michigan Library, 2009.
- [26] Chunming Zhao, Robert J. Baxley, G. Tong Zhou, Deepak Boppana, and J. Stevenson Kenney. Constrained clipping for crest factor reduction in multiple-user ofdm. In *Radio and Wireless Symposium, 2007 IEEE*, pages 341 –344, 2007.